THE UNIVERSITY *of* EDINBURGH

Edinburgh Research Explorer

UV and simulated solar photodegradation of 17-ethynylestradiol in secondary-treated wastewater by hydrogen peroxide or iron addition

OPEN ACCESS

UV and simulated solar photodegradation of 17α-ethynylestradiol in secondary-treated wastewater by hydrogen peroxide or iron addition

Zacharias Frontistis[1], Matheos Kouramanos[2], Spyridon Moraitis[2], Efthalia Chatzisymeon[3*], Evroula Hapeshi[4], Despo Fatta-Kassinos[4], Nikolaos P. Xekoukoulotakis[2], Dionissios Mantzavinos[1**]

(1) Department of Chemical Engineering, University of Patras, Caratheodory 1, University Campus, GR-26504 Patras, Greece

(2) School of Environmental Engineering, Technical University of Crete, GR-73100 Chania, Greece

(3) Institute for Infrastructure and Environment, School of Engineering, The University of Edinburgh, Edinburgh EH9 3JL, United Kingdom

(4) Civil and Environmental Engineering Department and Nireas, International Water Research Center, University of Cyprus, P.O. Box 20537, 1678, Nicosia, Cyprus.

*Corresponding author:
Email: e.chatzisymeon@ed.ac.uk, Tel: +44(0)1316505711, Fax: 44(0)1316506554
** Corresponding author:
Email: mantzavinos@chemeng.upatras.gr, Tel: +302610996136, Fax: +302610969532

1 **Abstract**

2 The extensive use of estrogens and their release, through various pathways, into the

3 environment, constitutes an emerging environmental problem that poses serious threats onto

4 public health. In this work the efficiency of UVC/H_2O_2 and $solar/Fe^{2+}$ treatment to degrade

5 17α-ethynylestradiol (EE2) in environmentally relevant concentrations of 100 μg/L in

6 secondary-treated wastewater matrices was investigated. Also, photolytic treatment was

7 performed under different irradiation sources, namely UVC, UVA and simulated solar light.

8 The effect of H_2O_2 (0 − 20 mg/L) and Fe^{2+} (0 − 15 mg/L) concentration was investigated and,

9 at optimal operating parameters, EE2 removal was 100% after 15 min of UVC/H_2O_2

10 treatment, while EE2 removal reached 86% after 60 min of $solar/Fe^{2+}$ treatment. In addition,

11 the effect of water matrix and pH was studied. Total organic carbon (TOC) and yeast

12 estrogen screening (YES) measurements showed the formation of stable intermediate

13 products during EE2 treatment and an attempt to elucidate the reaction pathways and

14 mechanisms through the identification of transformation products (TPs) by means of UPLC−

15 MS/MS was made. Several TPs, including quinone methide and 1,2-quinone derivatives,

16 were identified and competing pathways were suggested, in which hydroxylation, alkylation,

17 dealkylation, demethylation and dehydroxylation, amongst others were described as major

18 transformation mechanisms.

19

20 **Keywords:** wastewater; UVC; solar; estrogen; transformation products; pathways

21

1. Introduction

Endocrine disrupting compounds (EDCs) is an emerging environmental issue that poses serious threats to human beings. EDCs have the ability to interact with the endocrine system of organisms and either mimic or inhibit the action of animal endogenous hormones, thus leading to a variety of developmental and reproductive disorders, as well as feminizing effects [1]. Estrogens include natural, synthetic, and phyto-estrogens and are well-known EDCs. Of them, synthetic estrogens, such as 17α-ethynylestradiol (EE2), which is the basic component of the contraceptive pill, are generally more stable than natural estrogens in aqueous environment and have greater estrogenic potency (approx. 11−27 times) than the natural estrone (E1) and estradiol (E2) [2]. Recent in vivo studies showed that EE2 even in the order of μg/L was able to affect continuously exposed rats, by decreasing their bodyweight, accelerating vaginal opening, and altering estrous cycles in young animals [3]. Also, chronic exposure to environmentally relevant concentrations of EE2 could cause liver and gill lesions in zebrafish [4], depress gonadal growth in males mummichogs [5], and could affect the pituitary transcriptome in female salmons in previtellogenic stages of ovarian growth, altering the expression of hundreds of genes involved [6].

EE2 can enter into aqueous environments (i.e. surface and ground water bodies) through several pathways, such as wastewater treatment plants (WWTPs), septic systems, and after use in agriculture [7]. Besides, EE2 is resistant to biological oxidation and escapes intact from conventional WWTPs, thus accumulating in the environment [8]. Several studies have reported the occurrence of EE2 in WWTP effluents worldwide (in the range of ng/L), while even more studies have detected EE2 at surface and drinking water raising serious concerns for public health [7, 8]. All these findings indicate that current treatment processes at WWTPs are inadequate to completely remove EE2. Hence, additional or alternative processes should be applied to support existing WWTP and increase their efficiency.

Due to the effectiveness of UV light for disinfecting drinking water, many water treatment plants are installing UV based systems. Such UV systems may also be effective for treatment of chemical contaminants, although their ability to destruct them completely is still under investigation. Nasuhoglu et al. [9] reported that EE2 can be degraded by about 90% and 50% in pure water and in industrial wastewater matrices, respectively, after 30 min of UVC treatment. Other studies also showed that UVC has the potential to effectively destruct EE2 in the order of mg/L by UVC [10-12], UVC/TiO_2 [11], UVC/H_2O_2 [12, 13] or UV/Fe^{3+} [10] systems. However, more work has to be done to further optimize UV process and assess its efficiency to treat environmentally relevant EE2 concentrations in real wastewater matrices.

Another effective, low-cost and robust alternative that can be used as an additional or as a tertiary treatment in existing WWTPs, is the use of solar-driven photocatalytic processes. These seem to be the most suitable treatment technology for using natural sunlight; an abundant and free source of energy [14]. The role of iron in environmental chemistry was first reported in the 1990s and since then, several studies on the photo-assisted Fe^{2+}, mainly in the form of the Fenton reagent (i.e. Fe^{2+}/H_2O_2), for water treatment applications were published [14]. Iron can play a dominant catalytic role in organics degradation under natural environmental conditions. Also, iron is an abundant and non-toxic element and it can be found at concentrations between 0.5 and 50 mg/L in natural fresh waters, while it does not present a hazard to human health at levels up to 2 mg/L in drinking water [15]. The decomposition of EE2 by photo-Fenton process under simulated solar irradiation has been studied by Frontistis et al. [15] who found that solar photo-Fenton (5 mg/L Fe^{2+}/8.6 mg/L H_2O_2) treatment could completely remove 70 μg/L EE2 from wastewater matrix after only 6 min of treatment. Moreover, estrogens degradation by UV/Fe^{3+} [10] treatment system was studied and showed that the addition of iron can significantly enhance photolytic processes.

The aim of this work is to investigate the degradation of EE2 by UVC and solar irradiation. Environmentally relevant EE2 concentrations at the μg/L level are used, while emphasis is given on EE2 degradation in secondary-treated WWTP effluents. Additional materials, such as H_2O_2 and Fe^{2+} to support the photolytic process are used and operating parameters, including pH, EE2 initial concentration, concentration of peroxide or iron, water matrix and treatment time are investigated. In addition, transformation products are identified and potential EE2 degradation pathways are proposed. It should be noted that up to now, a limited number of studies exist with regard to the transformation products of EE2 [16-20] and that the photocatalytic degradation of EE2 proves to be a quite complex process due to the stable structure of the molecule even against such powerful oxidation processes.

2. Materials and Methods

For this work, 17α-ethynylestradiol (EE2) (>98%, Fluka), H_2O_2 (35% w/w, Merck) and humic acid (Sigma-Aldrich, CAS number: 57-63-6) were purchased and used as received. EE2 (chemical formula: $C_{20}H_{24}O_2$) is a white to creamy white, odourless crystalline powder with a molecular mass of 296.40 g/mol and its chemical structure is shown in Figure 1. Its solubility in water is 9.20 ± 0.09 mg·L^{-1} at 25.0 ± 0.5 °C [21] and its octanol-water partitioning coefficient (K_{ow}) is 3.67 [22]. To add, EE2 in distilled water has a maximum absorbance in UV-Vis electromagnetic spectrum at 221 nm [16].

1   Fe^{2+} is added in the aqueous solutions in the form of $FeSO_4 \cdot 7H_2O$ (≥99%, Sigma-Aldrich).

2   The wastewater (WW) matrix is collected from the outlet of the secondary treatment of the

3   municipal WWTP of Chania, Greece. The effluent's TOC content is 7.8 mg/L, its inherent

4   pH is about 8 and its conductivity is 820 µS/cm. Ultrapure water (UPW) at pH = 6.1 is taken

5   from a water purification system (EASYpureRF – Barnstead/Thermolyne, USA).

6   Commercially available bottled water is used as the drinking water matrix for this study.

7

8   Figure 1

9

10   In each photocatalytic run, 300 mL of the water matrix spiked with the appropriate amount of

11   EE2 and other chemical substances if required, are fed in the photochemical reactor.

12   Magnetic stirring is always provided and temperature is kept constant at $25\pm2\,^{o}C$, while the

13   reactor is open to the atmosphere. In those cases when hydrogen peroxide was used, residual

14   H_2O_2 was scavenged, in withdrawn samples, adding the appropriate amount of Na_2SO_3

15   (≥98%, Sigma-Aldrich).

16   UVA and UVC experiments are conducted in an immersion well, batch type, laboratory scale

17   photoreactor, purchased from Ace Glass (Vineland, NJ, USA) which is described in detail

18   elsewhere [23]. UVA irradiation is provided by a 9 W lamp (Radium Ralutec, 9W/78, 350–

19   400 nm). UVC irradiation is provided by an 11 W low pressure mercury lamp (Phillips, TUV

20   PL-S). The photon fluxes of the UV lamps are determined actinometrically using the

21   potassium ferrioxalate method and they are estimated at 4.69×10^{-6} einstein/s and 7.15×10^{-6}

22   einstein/s for the UVA and UVC lamp, respectively. Simulated solar irradiation is emitted by

23   a Newport 96000-150 Watt solar simulator system. Light source is placed on top of a double-

24   walled cylindrical pyrex cell containing the aqueous reactant mixture. The photon flux of the

25   solar lamp was measured using 2-nitrobenzaldehyde (purchased from Sigma–Aldrich) as the

26   chemical actinometer [24] and it was found to be 17.4×10^{-8} einstein/s.

27   Changes in EE2 concentration are followed by an HPLC (Alliance 2690, Waters) system

28   where separation is achieved on a Luna C-18(2) column (5 µm, 250 mm × 4.6 mm) and a

29   security guard column (4 mm×3 mm), both purchased from Phenomenex. Detection is

30   achieved through a fluorescence detector (Waters 474) and method details are described in

31   detail elsewhere [15]. Analyses of transformation products (TPs) of EE2 photodegradation

32   were performed by ultra performance liquid chromatography coupled with tandem mass

33   spectrometry on an ACQUITY TQD UPLC-MS/MS system (Waters) by a method described

34   in detail elsewhere [16]. Sample extraction was performed by solid phase extraction (SPE)

using cartridges built of hydrophilic and a lipophilic monomer (Oasis-HLB; 50 mg/3mL), and purchased from Waters (Milford, MA, USA). The sample (10 mL) is filtered through a syringe-filter (22 μm pores) prior to the SPE. TOC is measured on a Shimadzu 5050A TOC analyzer. EE2 absorbance spectrum is measured on a Shimadzu UV-Vis 1240 spectrophotometer. Residual H_2O_2 concentration was monitored using Merck peroxide test strips in the range 0–25 mg/L. Finally, the *in vitro* yeast estrogen screen (YES) bioassay was employed to assess estrogenic activity of the effluent before, and after treatment [15].

3. Results and Discussion

3.1. Irradiation source

The effect of the type of the irradiation is investigated using three different illumination systems, namely UVC, UVA and simulated solar irradiation. The results in Figure 2 show that the extent of the EE2 degradation follows the order of UVC > UVA > solar. Specifically, EE2 removal is 47%, 17% and 2% under UVC, UVA and solar irradiation, respectively after 60 min. In general, photolysis can occur by two ways; (i) directly through light absorption by the organic molecules, and (ii) indirectly when photosensitizers, such as TOC, absorb the light and generate reactive oxidant species (ROS) that promote molecule degradation [25]. In this work, the higher EE2 removal percentage under UVC irradiation can be explained both by its direct and indirect photolytic degradation. Firstly, the emission spectra of the lamps and the absorbance spectrum of EE2 should be taken into consideration. Measurements (data not shown) of the UV-Vis spectrum of EE2 show that it absorbs in the 200-300 nm range, with two significant absorption peaks at 230 nm and 280 nm. The UVC lamp emits at 254 nm, the UVA lamp emits in the 350 – 400 nm range (max. emission at 365 nm), and the solar irradiation consists of only about 5% of UVA (i.e. 300 – 500 nm) radiation, while the rest 95% illuminates in the Vis-IR electromagnetic spectrum. Therefore, only the UVC lamp emits in the absorbance spectrum of EE2, thus initiating its direct photolysis. Besides, indirect photolysis also takes place since all experiments, shown in Figure 2, are carried out in WW matrix with a TOC content of 7.8 mg/L. TOC can absorb UV irradiation and form ROS, thus enhancing EE2 degradation.

Moreover, the high performance of the UVC system can be also attributed to the higher photon flux that finally reaches the reactant solution. As the photon flux in the solution increases, the amount of photo-generated ROS in the effluent will be increased as well. In this work, the measured photon fluxes (shown in brackets) of the lamps follow the order of UVC (7.15×10^{-6} einstein/s) > UVA (4.69×10^{-6} einstein/s) > solar (17.4×10^{-8} einstein/s),

6

indicating the key role of photons' amount in the photolytic process. It should be noted that the geometrical characteristics of the photo-reactors can significantly affect the process efficiency. This is evident in this work, where fully immersed designs (i.e. UVC and UVA systems) allow optimal photon flux diffusion into the solution, while when the lamp is placed on top of the liquid, such as in the case of solar irradiation, the amount of photon flux in the solution is less than for the other illumination systems.

Further experiments are focused on the use of both UVC, which is already a widely applied disinfection technique in WWTPs, and on solar irradiation, a free and renewable source of energy, to explore the possibility of establishing a more sustainable and advanced treatment process in existing WWTPs.

Figure 2

3.2. UVC/H_2O_2 treatment

To enhance the EE2 degradation extent under UVC irradiation, the addition of $1 - 20$ mg/L H_2O_2 in WW is investigated and the results are shown in Figure 3. As can be seen, EE2 is completely and rapidly destructed after only 15 min of treatment, in the presence of 10 mg/L H_2O_2. Also, it is observed that the presence of hydrogen peroxide up to 10 mg/L could significantly enhance the degradation of EE2, while further increase of its concentration to 20 mg/L does not significantly affect process efficiency. Similar findings have been reported by other studies [15, 26, 27], yet the investigation of hydrogen peroxide addition in environmentally relevant EE2 matrices, under UVC irradiation, had been a missing element in literature. In general, hydrogen peroxide is expected to promote UVC photolysis as it absorbs in the range of $200 - 290$ nm and yields hydroxyl radicals which could then enhance EE2 indirect photolytic degradation [23, 26]. On the other hand, hydrogen peroxide can also react with hydroxyl radicals, thus scavenging the photo-generated ROS in the effluent that would otherwise be available for EE2 destruction. This phenomenon is likely to occur to an appreciable extent at increased H_2O_2 loadings and can explain the almost stable EE2 removal observed at 20 mg/L H_2O_2 concentration. It should be noted that a significant amount of H_2O_2 was consumed during the process since its residual concentration was 2 and 5 mg/L after the end of treatment, when the initial H_2O_2 loading was 10 mg/L and 20 mg/L, respectively. Therefore, all subsequent experiments under UVC irradiation were performed in the presence of 10 mg/L H_2O_2.

1

2   Figure 3

3

4   To get a better understanding of the EE2 degradation during UVC/H_2O_2 treatment, the effect

5   of initial EE2 concentration (50 – 200 µg/L) on the process efficiency is investigated.

6   Concentration – time profiles are followed (data not shown) and it is observed that the

7   reaction followed a pseudo-first-order rate expression. Specifically, after only 10 min of

8   UVC/H_2O_2 treatment at 10 mg/L H_2O_2, EE2 removal is 100%, 92% and 82% when initial

9   EE2 concentration is 50 µg/L, 100 µg/L and 200 µg/L, respectively. Besides, the respective

10 apparent k values are 0.293 min^{-1} (r^2=0.995), 0.247 min^{-1} (r^2=0.98) and 0.179 min^{-1}

11 (r^2=0.983).

12

13 **3.3. Solar/Fe^{2+} treatment**

14 Solar irradiation is currently promoted for water treatment since it is a cheap and renewable

15 source of energy and it has been used both for bacteria inactivation [28] and water

16 decontamination [29]. Yet, and as shown in Figure 2, solar irradiation alone cannot compete,

17 in terms of its effectiveness, with other photolytic processes. In addition, ferrous ion in acidic

18 aqueous solutions can be photolyzed under appropriate irradiation to produce hydroxyl

19 radicals and other strong non-selective oxidants [10]. These radicals may react with EE2, thus

20 enhancing its degradation as well as oxidizing the natural organic matter (NOM) present in

21 WW matrices. To investigate this, experiments are carried out under solar irradiation while

22 adding up to 15 mg/L Fe^{2+} in WW at pH=3, in order to avoid iron precipitation [10]. The

23 results are shown in Figure 4. It is observed that the addition of iron can significantly

24 promote the 60-min photodegradation of EE2 at 26%, 36%, 46% and 86%, in the presence of

25 1 mg/L, 2.5 mg/L, 5 mg/L and 15 mg/L Fe^{2+}. Therefore, solar/Fe^{2+} photocatalytic oxidation

26 might be an attractive method to increase the effectiveness of the solar photolytic process. In

27 addition, a final experiment was carried out in the presence of 5 mg/L Fe^{2+} and 10 mg/L H_2O_2

28 to assess the efficacy of the solar photo-Fenton process to remove 100 µg/L EE2 from treated

29 WW. It is observed that after only 15-30 min of treatment, EE2 is completely degraded, while

30 in the absence of H_2O_2 the respective EE2 removal is only 35%. As expected, solar photo-

31 Fenton can rapidly destruct EE2, yet for large-scale applications photo-Fenton might be non-

32 sustainable since it requires the addition of two chemical reagents to support the process.

33

34   Figure 4

Furthermore, a series of experiments at different EE2 concentrations are performed under solar irradiation and in the presence of 5 mg/L Fe^{2+} (data not shown). Conversion decreases with increasing EE2 concentration, i.e. the 60-min value was 53%, 46% and 38% at 50 μg/L, 100 μg/L and 200 μg/L EE2 concentration, respectively.

3.4. Effect of the water matrix

The use of ultrapure water solutions to simulate natural aqueous matrices is often a limitation of most laboratory studies. This is because natural waters contain dissolved and suspended substances, coming from animal and plant materials break down and usually referred to as NOM. The presence of NOM and of other inorganic substances can affect estrogens' photo-degradation either positively or, most commonly, negatively [24, 25, 30]. Therefore, in this work the effect of water matrix onto 100 μg/L EE2 degradation is investigated both for solar/Fe^{2+} and UVC/H_2O_2 treatments (Figure 5). Experiments are performed in several water matrices, such as ultrapure water (UPW), secondary-treated wastewater (WW), 10 mg/L humic acid (HA) solution (HA is one of the main NOM components) and a 50:50 mixture of WW:UPW. Firstly, it should be reported that EE2 photolytic degradation, under either solar (without iron) and UVC (without peroxide) irradiation, is almost negligible, at approximately 5-14% (data not shown) for all the experimental conditions (i.e. 15 min under UVC or 60 min under solar irradiation) described in Figure 5. Moreover, it was observed that TOC removal of WW, in the presence of EE2 which barely contributes to total TOC, was always below 10% (data not shown) for both UVC/H_2O_2 and solar/Fe^{2+} treatment (i.e. for the experimental conditions shown in Figures 3 and 4). The almost negligible TOC removal shows the highly recalcitrant nature of the real WW matrix.

Figure 5

As can be seen in Figure 5a, water matrix affects the process efficiency at least at the initial stages of oxidation. More specifically, EE2 removal is lower in WW and in HA than in UPW matrix. Interestingly in all cases EE2 is completely removed after 15 min of UVC/H_2O_2 treatment showing the capacity of this process to destruct recalcitrant micro-contaminants, such as EE2, in WWTP effluents. Figure 5b shows that EE2 removal is decreased in complex

9

water matrices as this is 78%, 70%, 59%, and 46% in UPW, drinking, HA, and WW matrix, respectively, after 60 min of solar/Fe^{2+} treatment. Similar results were found during the heterogeneous photocatalytic degradation of EDCs [16, 24, 31]. This is due to the fact that the non-selective photo-generated ROS are competitively consumed by the NOM present in treated WW, which contains 7.8 mg/L of TOC. Since NOM is known to be refractory to biological or chemical oxidation and constitutes most of the matrix's total organic content, non-selective oxidizing agents will partly be wasted attacking this fraction [31], thus reducing the degradation rate of the target compound. Also, hydroxyl radicals may be scavenged by bicarbonates and chlorides present in WW or HA to form other ROS, whose oxidation potential is lower than that of the hydroxyl radicals [32].

3.5. Effect of pH

The effect of pH on the process efficiency is studied and a series of experiments are carried out at pH values of 3, 5 and 8 to destruct 100 µg/L EE2 in treated WW. The results are shown in Figure 6. It is observed (Figure 6a) that increased pH values can increase the degradation efficiency of the UVC/H_2O_2 treatment achieving 92%, 82% and 67% EE2 removal after 10 min at pH values of 8 (i.e. effluents' ambient pH), 5 and 3, respectively. These results are consistent with those obtained in other studies [33], where a pH increase from 5 to 8 led to a substantial increase of EE2 photolytic removal, indicating that changes in pH may affect the formation rate of reactive oxygen species. Undeniably, the higher EE2 removal at pH 8, which is the ambient pH of natural water bodies, is an additional benefit to the utilization of UVC/H_2O_2 treatment for EE2 removal in WW matrix. On the other hand, solar/Fe^{2+} process efficiency is enhanced at low pH values (Figure 6b), i.e. EE2 degradation is 17%, 32% and 46% at pH values equal to 8, 5 and 3, respectively. These findings are consistent with other studies [10] and this is due to the fact that iron precipitates at pH>4, and therefore less amount of soluble iron is available to produce hydroxyl radicals for EE2 oxidation. Also, bicarbonates, well known radical scavengers, at pH 3 may be transformed into gaseous phase as CO_2, which is eventually emitted to atmosphere, thus allowing more radicals to oxidize the target compounds.

Figure 6

3.6. Mineralization and estrogenicity removal

For the various experiments performed in this work, changes in TOC were monitored alongside EE2 conversion. For the UVC/H_2O_2 system, TOC reduction never exceeded 11%, and this is even lower (6%) for the solar/Fe^{2+} system. These results clearly show that although EE2 is degraded, other very recalcitrant intermediate organic products are generated either from EE2 cleavage or from DOC degradation. Not only this, but measurements of the effluent's estrogenic activity showed that although complete estrogen degradation is achieved after 15 min of UVC/H_2O_2 treatment (Figure 3), this is accompanied by a partial estrogenicity removal of just 35%. These results show that the photolytic transformation of EE2, as well as that of the wastewater organic matter, can generate certain stable by-products that are estrogenically potent and responsible for most of the remaining estrogenicity. Similar discrepancies between estrogen and estrogenicity removal during treatment by photo-Fenton oxidation or heterogeneous photocatalysis have been recently reported [15, 33].

3.7. Formation of TPs and proposed transformation pathways of EE2

3.7.1. Solar/Fe^{2+} process

Figure 7a illustrates the postulated chemical structures and the exact mass values of the detected ions for the degradation products identified, during the EE2 solar/Fe^{2+} degradation process. Overall, the screening of the treated samples allowed to tentatively identify the formation of fourteen TPs (TP1-TP14), with their peaks being greater than 15% of the highest peak intensity. Even though transformation mechanisms similar to those suggested by other studies, are proposed herein, some transformation products have not been previously reported, indicating that a plethora of TPs may occur depending on the experimental and analytical set up. The structure of most TPs of EE2 shows preservation of the core structure of the estrogens which can potentially explain the remaining estrogenicity after treatment or at least part of it. TP1 with m/z 301 (RI 30-70%) is possibly formed from the addition of four hydrogen atoms to EE2. TP2 (181 m/z, RI 20-80%) and TP3 (149 m/z, RI 15-55%) are formed from the cleavage of C-C bond from the main structure of EE2, in accordance to the transformation pathway of EE2. Therefore, the elucidation of these possible structures of TPs could also result in the removal of few carbon atoms from the hydrocarbon side chains. The formation of TP2 and TP3 indicates the cleavage of the C11-C12 and C9-C10 bond of EE2 as a preferential route, which was originated from a series of C–C cleavage products such as the formation of 2,4a,9,10-tetrahydrophenanthrene and 5,6,7,8-tetrahydro-2-naphthol (THN), respectively. More specifically, TP2 and TP3 can be formed by the combination of the

dehydroxylation, demethylation at the position C12 and finally abstraction of alkyl group, cyclopentane and octahydro-1H-indene, respectively. The THN molecule was previously used as a model for steroid hormone photodegradation studies [17, 34]. TP3 can be formed through two reaction routes of EE2→TP3 and EE2→TP2→TP3. TP3 can be directly formed from EE2 but can be also generated through two reactions, hydroxylation and abstraction of cyclohexa-1,4-diene of the TP2. For this reason, TP2 can be regarded as the promoter for the formation of TP3 (m/z 149). In this study, TP6, TP11 and TP12 are some of the major transformation products formed after the treatment, which may be attributed to the hydroxylation of EE2. Several isobaric compounds (polyhydroxylated compounds), corresponding to positional isomers, may be formed. However, differentiation of positional isomers was not always feasible based solely on the UPLC-MS/MS data. More specifically, the degradation of EE2 could lead to the formation of di-hydroxylated photoproducts (2-HO-EE2), TP6 (m/z 403), TP11 (m/z 329) and TP12 (m/z 305). As previously observed by Frontistis et al. [33] during the TiO$_2$ photocatalytic degradation of EE2 one of the major TPs was TP11 with 329 m/z (RI 15-60%), which may be generated after di-hydroxylation of the aromatic ring, whose further loss the ethynyl moiety would yield TP12 (m/z 305, RI 40-80%). The formation of dihydroxy photoproducts, 2-HO-EE2, possibly comes from the attack of hydroxyl radicals on the aromatic rings [16, 17, 33] [18]. Nevertheless, it is worth mentioning that TP11 and TP12 are the most frequently identified oxidation TPs of E2 and EE2 using various advanced oxidation processes [16, 33, 35]. In contrast, the analogous photoproduct with 329 m/z which may be formed with direct attack of OOH radicals and the photoproduct with 327 m/z which can be formed with abstraction of two hydrogen atoms were not observed, as previously reported [16, 19, 20]. TP6 can be formed through the reaction route of EE2→TP5→TP6. The elucidation route of TP6 can be attributed to the di-hydroxylation, abstraction methyl group at C-11 of the structure and finally further addition of hydrogen atoms at ethynyl group of the TP5.

Dealkylation is one of the major photooxidation mechanisms that it is observed in the present study. In contrast with Mazellier et al. [17], TP13 (m/z 273, RI 30-100%) may be formed with abstraction of alkyl group at position C17, whose further reduction would yield TP14 (m/z 271, RI 40-80%).

Alkylation of the aliphatic ring of EE2 also occurs resulting in the formation of five major analogues of EE2, TP5 (m/z 351, RI 15-50%), TP7 (m/z 449, RI 25-45%), TP8 (m/z 337, RI 15-60%), TP9 (m/z 493, RI 20-55%) and TP10 (B) (377 m/z, RI=15-50%). The formation of these photoproducts may be attributed to the alkylation on the one of the aliphatic ring at C-7

and C-8 positions and elimination of the hydrogen atoms, while TP7 can be generated by the combination of demethylation at the position C12, and finally alkylation at position C-7 and C-8 through TP6. Finally, another analogue, TP4 (m/z 227, RI=25-55%) contains multiple structural changes consistent with the ethynyl moiety liberation at the position C-17 of the structure together with demethylation and dehydroxylation processes.

Figure 7

3.7.2. UVC/H$_2$O$_2$ process

Figure 7b presents the eleven TPs (TP1*-TP11*) identified and the proposed reaction pathway of EE2 degradation during the UVC photolytic treatment. Six of the eleven proposed TPs (TP2*, TP5*-TP8*, TP10*) are the same with those observed during the solar/Fe^{2+} treatment.

Several TPs (TP1*(A)-(B), TP7* and TP9*) are formed through the hydroxylation step. TP1(A)* (m/z 331), TP1*(B) (m/z 331), TP7*(m/z 403) and TP9* (m/z 314) are the major transformation products formed during this mechanism. Subsequent hydroxyl radical addition could lead to the formation of mono- (TP1(B)*, m/z 331 and TP9*, m/z 314) and bihydroxylated (TP1*(A), m/z 331 and TP7*, m/z 403) products. As seen in Figure 7b, several isobaric compounds corresponding to positional isomers are detected. However, differentiation of positional isomers is not feasible based solely on the UPLC-MS/MS data. More specifically, TP1(A)* (m/z 331; RI 30-100%) can be formed through the loss of two hydrogen atoms and subsequent addition of two hydroxyl radicals onto the saturated ring linked to the aromatic one in the structure of EE2. TP1(B)* can be formed through two reaction routes of EE2→TP1(B)* and EE2→TP2*→TP1(B)*. TP1(B)* can be directly formed by the combination of monohydroxylation onto the saturated ring of the structure and methylation of EE2. In parallel to hydroxylation, methylation reactions are also demonstrated by the presence of protonated molecules with addition of hydrogen atoms at ethynyl moiety. TP1(B)* can be also generated through one-fold methylation and hydroxylation of the TP2, which can be regarded as the promoter for the formation of this photoproduct (m/z 331).

The formation of TP7* can occur through monohydroxylation and then by further addition of a methyl group of TP6*. The TP9* (m/z 314; RI 15-55%) can result from the direct attack of hydroxyl radical at position C-10 of the linked saturated ring on the EE2 structure forming monohydroxylate-derivative [33]. Chen et al. [36] reported that the frontier electron density value was higher for the carbon atoms at positions 3 and 10 of the aromatic ring of EE2, with

carbon at position 10 having the highest value of electron density of all the atoms in EE2. This finding is in perfect agreement with the value of the frontier electron density estimated by Ohko et al. [37], on the structurally similar E2 molecule. These values indicate that the most probable sites at which an electron would be abstracted by a hole are the carbon atoms at positions 3 and 10 of the aromatic ring of EE2. Given that there is relatively little steric hindrance to attack by electrophiles at the aromatic ring of EE2, it can be assumed that C-10 of the structure should be the most favorable site for electrophilic attack [33].

In addition to the assigned product ions, TP2* at 301 m/z is observed. Frontistis et al. [33] reported that the identified TP2* could be possibly generated through the addition of four hydrogen atoms to EE2.

Subsequently, UVC treatment of EE2 can lead to the formation of two other analogues of EE2 i.e. TP3*(A)-(B) with m/z values 251 and TP4* with m/z values 233. TP3*(B) (m/z 251; RI 15-30%) may be formed by cleavage of the aromatic ring of EE2, whose subsequent decarboxylation following by addition of ethynyl moiety at position C17 gives TP4*(m/z 233; RI 25-45%) which eventually leads to low molecular weight compounds, corresponding to aliphatic carboxylic acids and other ring-cleavage compounds. The other analogue, TP3(A)* (m/z 251; RI 15-30%), may be formed following two hydroxyl groups liberation, through C-1 and C-17 and losing methyl moiety from position 12.

UVC photolytic oxidation of EE2 can lead to the formation of four other TPs i.e. TP6* (m/z 361), TP8* (m/z 449), TP10* (m/z 493) and TP11* (m/z 361). As in the case of the solar/Fe^{2+} process, one of the major mechanisms is the alkylation of the aliphatic ring of EE2. TP6*(m/z 361, RI 20-40%), TP8* (m/z 449, RI 15-35%), TP10* (m/z 493, RI 20-60%) and TP11* (m/z 361, RI 25-70%) may be formed by alkylation at positions C7 and C8 on the aliphatic ring next to the saturated ring. TP8* may be formed through two reaction routes of EE2→TP6*→TP8* and EE2→TP6*→TP7*→TP8*. Through the second reaction route, photoproduct with 449 m/z may indicate possible abstraction of two hydroxyl groups, demethylation and finally addition of octahydro-1H-indene at positions 7 and 8 of TP7*. The formation of TP8* can be also attributed to the one-fold addition of octahydro-1H-indene group at C7-C8 and subsequent addition of hydrogen atoms at the ethynyl moiety.

Finally, according to the elucidation of EE2 pathway, TP5* (m/z 227; RI 25-75%) is created from EE2 after loss of hydroxyl radicals, loss of methyl group at position 12 and loss of the ethynyl moiety at C-17.

4. Conclusions

In this work, the fate of synthetic estrogen hormone EE2 is monitored under UVC irradiation or simulated solar light in the presence of iron in environmentally relevant matrices. The selection of these two systems is justified taking into account that (i) several WWTPs upgrade their disinfection procedures through installing UVC setups, and (ii) natural attenuation driven by sunlight and iron inherently present in WWTPs (and, indeed, other water courses) may occur. In a nutshell:

1) Although UVC alone can partly remove EE2 at the µg/L level, the extent of removal is substantially enhanced with the addition of H_2O_2 (which may also serve as disinfectant) at the low mg/L level; since EDCs are, in practice, present at the ng/L level, there may be no need for additional oxidants.

2) EE2 is susceptible to degradation by sunlight and iron; the process is sensitive to parameters such as the concentration of iron and the complexity of the water matrix.

3) The estrogenicity associated with the presence of EDCs in complex matrices may not be completely removed upon the elimination of specific estrogens. This brings forward the need to monitor the formation of key TPs and evaluate their biological potency. In this work, UPLC-MS/MS analysis is performed to identify such TPs and propose reaction mechanisms and pathways.

1   References

2

3   [1]   M. Yang, M.S. Park, H.S. Lee, Endocrine disrupting chemicals: Human exposure and

4   health risks, J Environ Sci Health C Environ Carcinog Ecotoxicol Rev 24 (2006) 183-

5   224.

6   [2]   S.A. Snyder, T.L. Keith, D.A. Verbrugge, E.M. Snyder, T.S. Gross, K. Kannan, J.P.

7   Giesy, Analytical Methods for Detection of Selected Estrogenic Compounds in

8   Aqueous Mixtures, Environ Sci Technol 33 (1999) 2814-2820.

9   [3]   K.B. Delclos, C.C. Weis, T.J. Bucci, G. Olson, P. Mellick, N. Sadovova, J.R.

10   Latendresse, B. Thorn, R.R. Newbold, Overlapping but distinct effects of genistein

11   and ethinyl estradiol (EE2) in female Sprague–Dawley rats in multigenerational

12   reproductive and chronic toxicity studies, Reprod Toxicol 27 (2009) 117-132.

13   [4]   N. Xu, P. Chen, L. Liu, Y. Zeng, H. Zhou, S. Li, Effects of combined exposure to

14   17α-ethynylestradiol and dibutyl phthalate on the growth and reproduction of adult

15   male zebrafish (Danio rerio), Ecotoxicol Environ Saf 107 (2014) 61-70.

16   [5]   E.G. Meina, A. Lister, T. Bosker, M. Servos, K. Munkittrick, D. MacLatchy, Effects

17   of 17α-ethynylestradiol (EE2) on reproductive endocrine status in mummichog

18   (Fundulus heteroclitus) under differing salinity and temperature conditions, Aquat

19   Toxicol 134–135 (2013) 92-103.

20   [6]   L.B. Harding, I.R. Schultz, G.W. Goetz, J.A. Luckenbach, G. Young, F.W. Goetz, P.

21   Swanson, High-throughput sequencing and pathway analysis reveal alteration of the

22   pituitary transcriptome by 17α-ethynylestradiol (EE2) in female coho salmon,

23   Oncorhynchus kisutch, Aquat Toxicol 142–143 (2013) 146-163.

24   [7]   A.Z. Aris, A.S. Shamsuddin, S.M. Praveena, Occurrence of 17α-ethynylestradiol

25   (EE2) in the environment and effect on exposed biota: a review, Environ Int 69

26   (2014) 104-119.

27   [8]   Y. Luo, W. Guo, H.H. Ngo, L.D. Nghiem, F.I. Hai, J. Zhang, S. Liang, X.C. Wang, A

28   review on the occurrence of micropollutants in the aquatic environment and their fate

29   and removal during wastewater treatment, Sci Total Environ 473–474 (2014) 619-

30   641.

31   [9]   D. Nasuhoglu, D. Berk, V. Yargeau, Photocatalytic removal of 17α-ethynylestradiol

32   (EE2) and levonorgestrel (LNG) from contraceptive pill manufacturing plant

33   wastewater under UVC radiation, Chem Eng J 185–186 (2012) 52-60.

[10] B. Liu, F. Wu, N.-s. Deng, UV-light induced photodegradation of 17α-ethynylestradiol in aqueous solutions, J Hazard Mater 98 (2003) 311-316.

[11] G. Li Puma, V. Puddu, H.K. Tsang, A. Gora, B. Toepfer, Photocatalytic oxidation of multicomponent mixtures of estrogens (estrone (E1), 17β-estradiol (E2), 17α-ethynylestradiol (EE2) and estriol (E3)) under UVA and UVC radiation: Photon absorption, quantum yields and rate constants independent of photon absorption, Appl Catal B 99 (2010) 388-397.

[12] E.J. Rosenfeldt, P.J. Chen, S. Kullman, K.G. Linden, Destruction of estrogenic activity in water using UV advanced oxidation, Sci Total Environ 377 (2007) 105-113.

[13] E.J. Rosenfeldt, K.G. Linden, Degradation of Endocrine Disrupting Chemicals Bisphenol A, Ethinyl Estradiol, and Estradiol during UV Photolysis and Advanced Oxidation Processes, Environ Sci Technol 38 (2004) 5476-5483.

[14] S. Malato, P. Fernández-Ibáñez, M.I. Maldonado, I. Oller, Chapter 15 - Solar Photocatalytic Processes: Water Decontamination and Disinfection, in: S.L. Suib, (Ed.), New and Future Developments in Catalysis, Elsevier, Amsterdam, 2013, pp. 371-393.

[15] Z. Frontistis, N.P. Xekoukoulotakis, E. Hapeshi, D. Venieri, D. Fatta-Kassinos, D. Mantzavinos, Fast degradation of estrogen hormones in environmental matrices by photo-Fenton oxidation under simulated solar radiation, Chem Eng J 178 (2011) 175-182.

[16] Z. Frontistis, V.M. Daskalaki, E. Hapeshi, C. Drosou, D. Fatta-Kassinos, N.P. Xekoukoulotakis, D. Mantzavinos, Photocatalytic (UV-A/TiO2) degradation of 17α-ethynylestradiol in environmental matrices: Experimental studies and artificial neural network modeling, Journal of Photochemistry and Photobiology A: Chemistry 240 (2012) 33-41.

[17] P. Mazellier, L. Méité, J.D. Laat, Photodegradation of the steroid hormones 17β-estradiol (E2) and 17α-ethinylestradiol (EE2) in dilute aqueous solution, Chemosphere 73 (2008) 1216-1223.

[18] Y. Zhao, I. Hu, W. Jin, Transformation of oxidation products and reduction of estrogenic activity of 17beta-estradiol by a heterogeneous photo-Fenton reaction, Environ Sci Technol 42 (2008) 5277-5284.

[19] B.E. Segmuller, B.L. Armstrong, R. Dunphy, A.R. Oyler, Identification of autoxidation and photodegradation products of ethynylestradiol by on-line HPLC-NMR and HPLC-S, J Pharm Biomed Anal 23 (2000) 927-937.

[20] J. Mai, W. Sun, L. Xiong, Y. Liu, J. Ni, Titanium dioxide mediated photocatalytic degradation of 17beta-estradiol in aqueous solution, Chemosphere 73 (2008) 600-606.

[21] A. Shareef, M.J. Angove, J.D. Wells, B.B. Johnson, Aqueous Solubilities of Estrone, 17β-Estradiol, 17α-Ethynylestradiol, and Bisphenol A, J Chem Eng Data 51 (2006) 879-881.

[22] Data from SRC PhysPropDatabase accessed via SRC's Fate Pointer File, http://esc.syrres.com/fatepointer/search.asp.

[23] A. Paleologou, H. Marakas, N.P. Xekoukoulotakis, A. Moya, Y. Vergara, N. Kalogerakis, P. Gikas, D. Mantzavinos, Disinfection of water and wastewater by TiO2 photocatalysis, sonolysis and UV-C irradiation, Catal Today 129 (2007) 136-142.

[24] V. Koutantou, M. Kostadima, E. Chatzisymeon, Z. Frontistis, V. Binas, D. Venieri, D. Mantzavinos, Solar photocatalytic decomposition of estrogens over immobilized zinc oxide, Catal Today 209 (2013) 66-73.

[25] C.P. Silva, M. Otero, V. Esteves, Processes for the elimination of estrogenic steroid hormones from water: A review, Environ Pollut 165 (2012) 38-58.

[26] E. Chatzisymeon, E. Stypas, S. Bousios, N.P. Xekoukoulotakis, D. Mantzavinos, Photocatalytic treatment of black table olive processing wastewater, J Hazard Mater 154 (2008) 1090-1097.

[27] S. Sarkar, S. Ali, L. Rehmann, G. Nakhla, M.B. Ray, Degradation of Estrone in Water and Wastewater by Various Advanced Oxidation Processes, J Hazard Mater.

[28] D. Rubio, E. Nebot, J.F. Casanueva, C. Pulgarin, Comparative effect of simulated solar light, UV, UV/H2O2 and photo-Fenton treatment (UV−Vis/H2O2/Fe2+,3+) in the Escherichia coli inactivation in artificial seawater, Water Res 47 (2013) 6367-6379.

[29] S. Malato, P. Fernández-Ibáñez, M.I. Maldonado, J. Blanco, W. Gernjak, Decontamination and disinfection of water by solar photocatalysis: Recent overview and trends, Catal Today 147 (2009) 1-59.

[30] N.P. Xekoukoulotakis, C. Drosou, C. Brebou, E. Chatzisymeon, E. Hapeshi, D. Fatta-Kassinos, D. Mantzavinos, Kinetics of UV-A/TiO2 photocatalytic degradation and

mineralization of the antibiotic sulfamethoxazole in aqueous matrices, Catalysis Today 161 (2011) 163-168.

[31] A. Zacharakis, E. Chatzisymeon, V. Binas, Z. Frontistis, D. Venieri, D. Mantzavinos, Solar photocatalytic degradation of bisphenol a on immobilized ZnO or TiO2, Int J Photoenergy 2013 (2013).

[32] C. Sirtori, A. Agüera, W. Gernjak, S. Malato, Effect of water-matrix composition on Trimethoprim solar photodegradation kinetics and pathways, Water Res 44 (2010) 2735-2744.

[33] Z. Frontistis, C. Drosou, K. Tyrovola, D. Mantzavinos, D. Fatta-Kassinos, D. Venieri, N.P. Xekoukoulotakis, Experimental and Modeling Studies of the Degradation of Estrogen Hormones in Aqueous TiO2 Suspensions under Simulated Solar Radiation, Ind Eng Chem Res 51 (2012) 16552-16563.

[34] M.M. Huber, T.A. Ternes, U. von Gunten, Removal of estrogenic activity and formation of oxidation products during ozonation of 17alpha-ethinylestradiol, Environ Sci Technol 38 (2004) 5177-5186.

[35] R.O. Pereira, C. Postigo, M.L. de Alda, L.A. Daniel, D. Barceló, Removal of estrogens through water disinfection processes and formation of by-products, Chemosphere 82 (2011) 789-799.

[36] J.L. Chen, S. Ravindran, S. Swift, L.J. Wright, N. Singhal, Catalytic oxidative degradation of 17alpha-ethinylestradiol by FeIII-TAML/H2O2: estrogenicities of the products of partial, and extensive oxidation, Water Res 46 (2012) 6309-6318.

[37] Y. Ohko, K. Iuchi, C. Niwa, T. Tatsuma, T. Nakashima, T. Iguchi, Y. Kubota, A. Fujishima, 17 beta-estradiol degradation by TiO2 photocatalysis as a means of reducing estrogenic activity, Environ Sci Technol 36 (2002) 4175-4181.
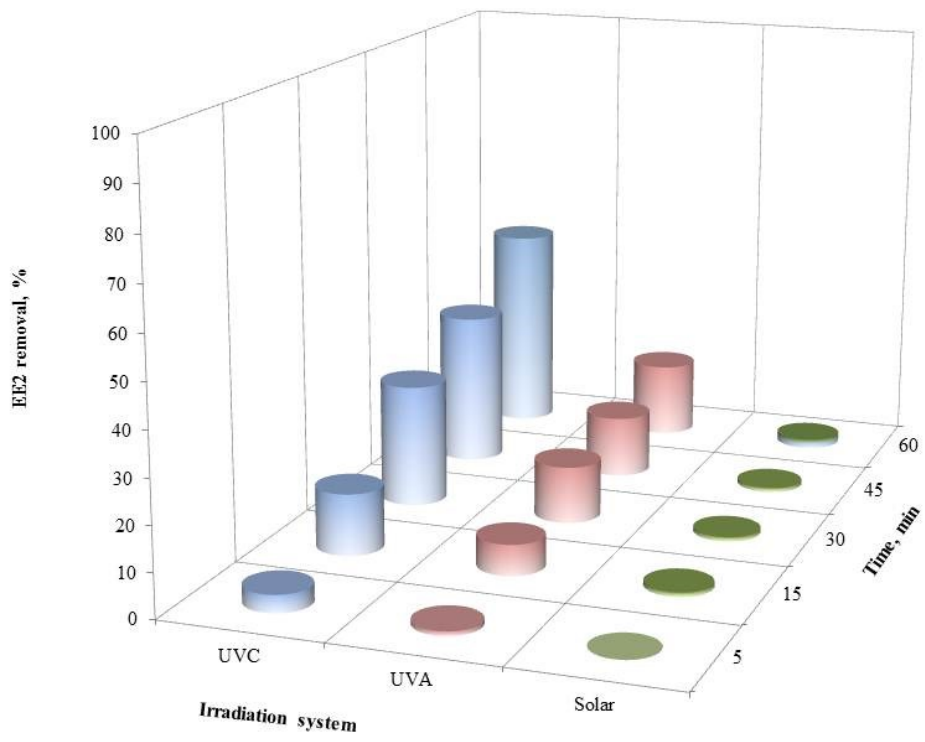
1

LIST OF FIGURES

17

1

2

3

4   Figure 1.
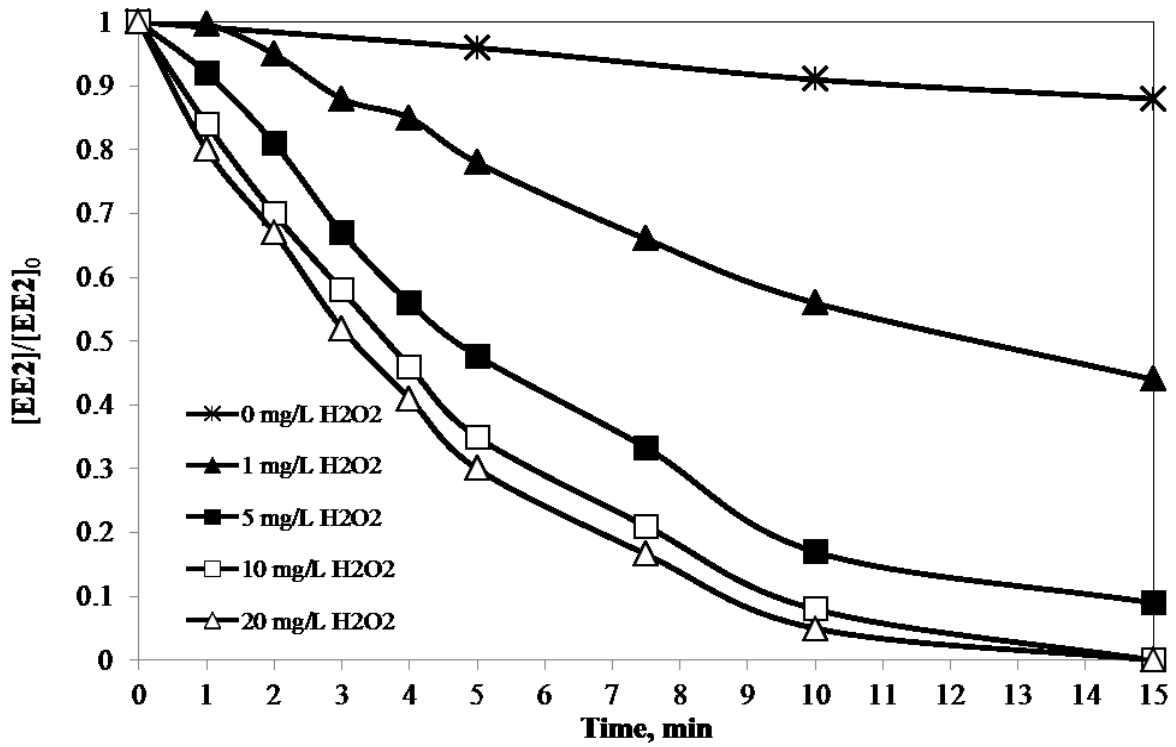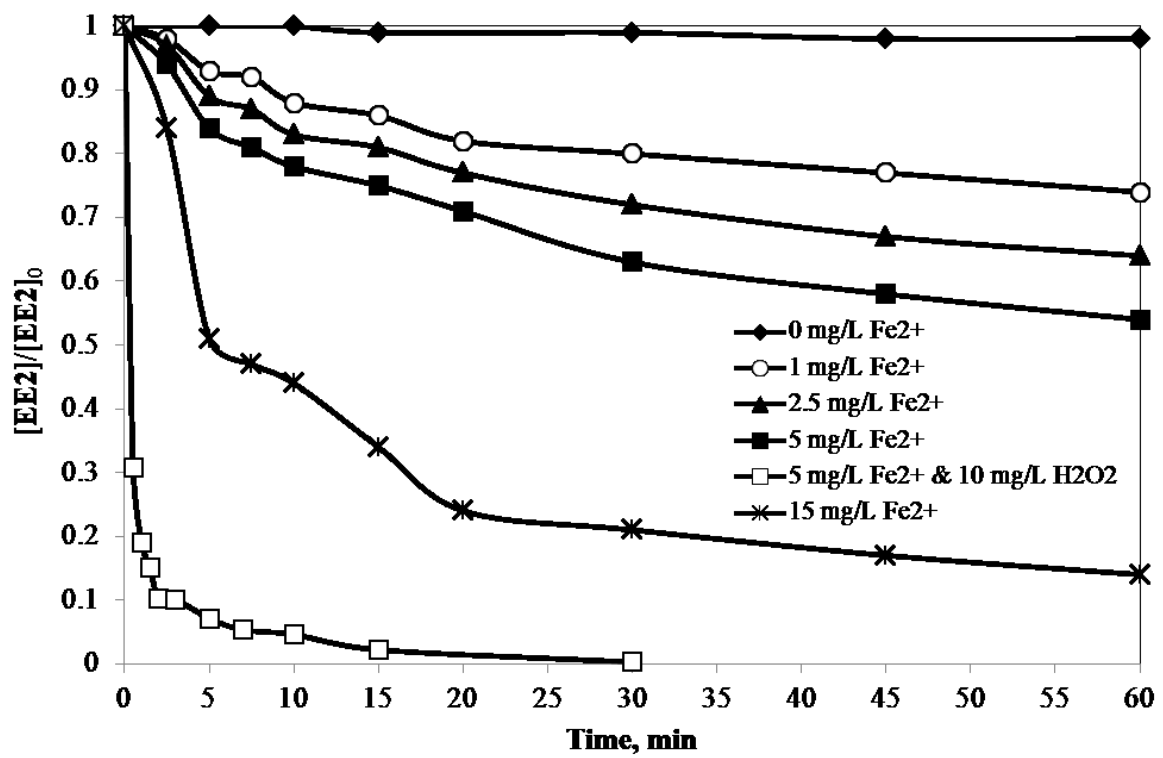
5

1

2   Figure 2.

3
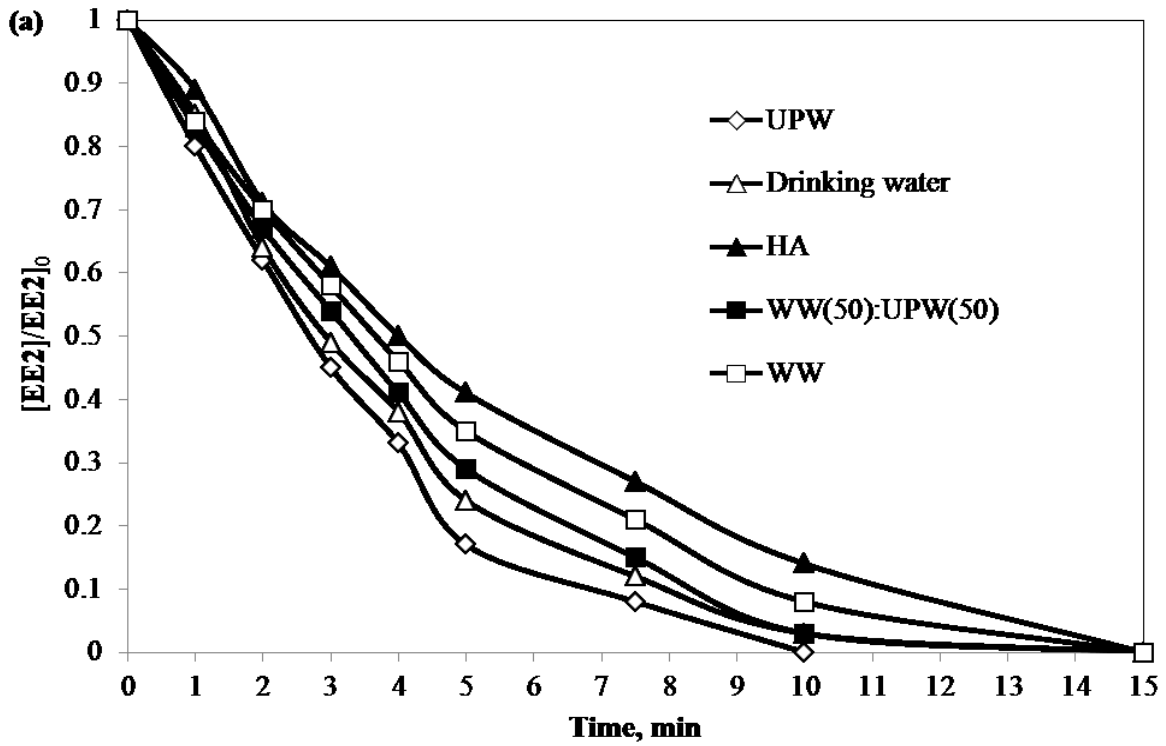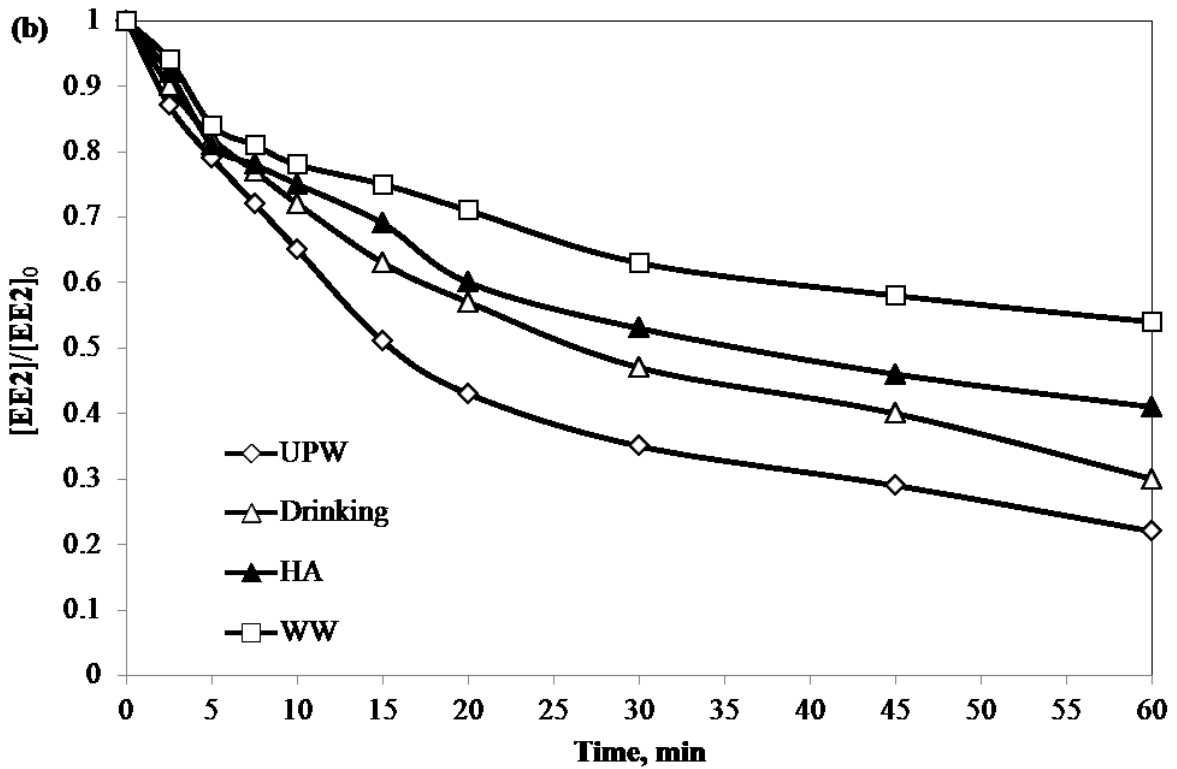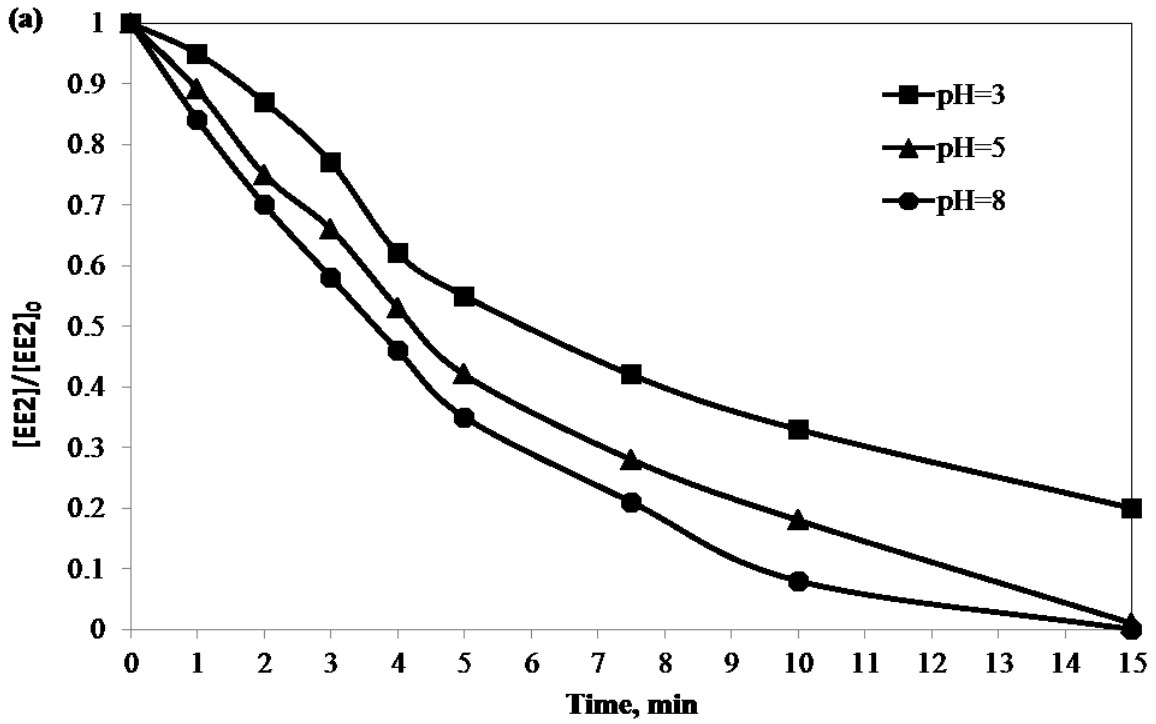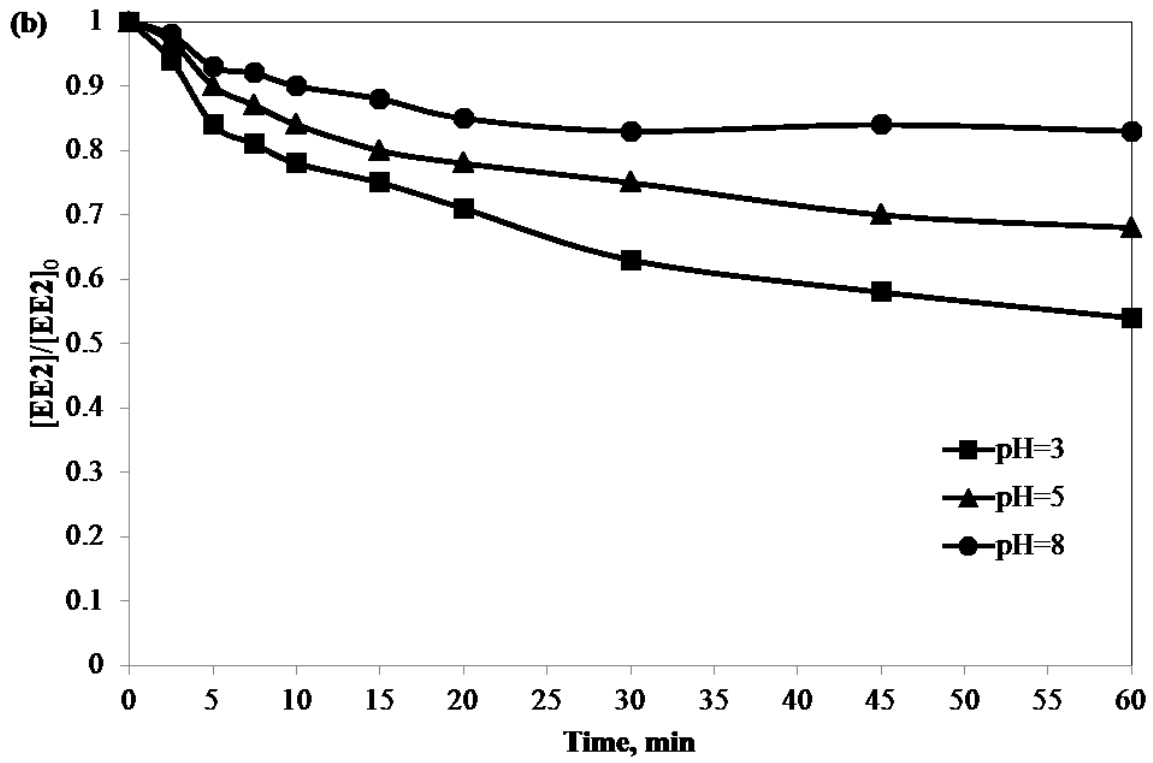
1

2   Figure 3.

3

4

5   Figure 4.

1

2

3

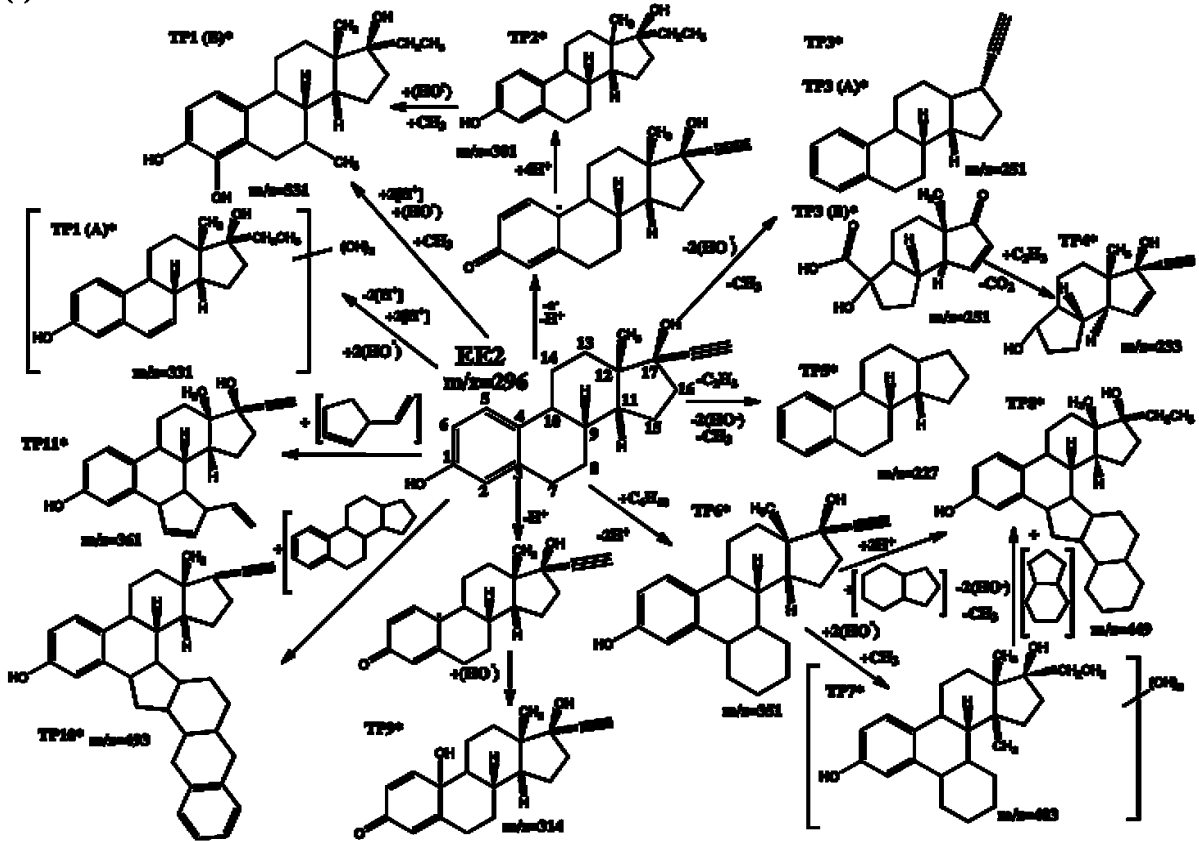4   Figure 5.

5

Figure 6.

1

2

3

(b)

Figure 7.